Highly efficient polarized GeS/$MoSe_2$ van der Waals heterostructure for water splitting under ultraviolet to near infrared light

Di Gu[1,2,3], Xiaoma Tao[1], Hongmei Chen[1], Weiling Zhu[3], Yifang Ouyang[1,], Yong Du[4], Qing Peng[5,*].*

[1] School of Physical Science and Technology, Guangxi University, Nanning 530004, People's Republic of China.
[2] School of Chemistry and Chemical Engineering, Guangxi University, Nanning 530004, People's Republic of China.
[3] Department of Physics, School of Science, Guangdong University of Petrochemical Technology, Maoming, Guangdong 525000, People's Republic of China.
[4] State Key Laboratory of Powder Metallurgy, Central South University, Changsha, 410083, China.
[5] Department of Nuclear Engineering and Radiological Science, University of Michigan, Ann Arbor, MI 48109, USA
[*] E-mail: ouyangyf@gxu.edu.cn(Y.O.) and qpeng.org@gmail.com (Q.P.)

High-efficient photocatalyst is critical for water splitting by solar light. Here we via first principles calculations propose the two dimension (2D) polarized GeS/$MoSe_2$ van der Waals (vdW) heterostructure for efficient water redox photocatalyst. The performance of GeS/$MoSe_2$ heterostructure is better than isolated materials, due to the properties of GeS monolayer and $MoSe_2$ monolayer are complementary by forming vdW heterostructure. GeS/$MoSe_2$ heterostructure possesses suitable band gap, dipole induced internal electric field and excellent solar absorption performance. The band alignments of GeS/$MoSe_2$ heterostructure are suitable compared with the redox potential of water. It is feasible to tune the opto-electronic properties and enhance photocatalytic activity of GeS/$MoSe_2$ heterostructure via strain engineering. Biaxial compressive strain range of -2% to -3% induces the direct band gap characteristic in GeS/$MoSe_2$ heterostructure. Our results suggest that 2D polarized GeS/$MoSe_2$ van der Waals heterostructure is a potential novel high-efficienct

Author Manuscript

This is the author manuscript accepted for publication and has undergone full peer review but has not been through the copyediting, typesetting, pagination and proofreading process, which may lead to differences between this version and the Version of Record. Please cite this article as doi: 10.1002/pssr.201900582

This article is protected by copyright. All rights reserved

photocatalyst for water splitting under a wide range of sunlight from ultraviolet to near-infrared.

Keywords: $GeS/MoSe_2$, polarized material, van der Waals heterostructure, water splitting

1. Introduction

Harvesting solar light is an ultimate solution to energy crisis. Photocatalytic water splitting technology, in which process solar light, water and catalyst are adopted to generate O_2 and H_2 without polluting the environment, has been considered as an efficient and feasible approach to solve the serious energy and environmental problems[1-3]. There are three major processes in photocatalytic water splitting, as the photo-generated electron-hole pairs separate and transfer to the surface of photocatalysts, and the H_2 (O_2) are generated by the way of hydrogen evolution reaction (oxygen evolution reaction) on the surface of photocatalysts, respectively[4, 5]. Therefore, effective solar light harvesting and carrier separation are keys to enhance the efficiency of photocatalytic water splitting process. Since Fujishima et al.[6] reported photocatalytic water splitting in 1972 firstly, bulk materials, such as TiO_2[7-10], ZnO[11, 12], CdS[13-15] and $SrTiO_3$[16, 17], have been extensively investigated as potential photocatalysts. However, the conversion efficiency of these bulk materials are still low and unsatisfactory due to the large band gap, low solar light absorption, low carrier mobility, and high carrier recombination rate[5, 18]. Compared to the traditional bulk materials, a series studies reported that two dimension (2D) materials have distinctive advantageous properties for photocatalytic water splitting, such as large specific surface area, short distance for charge carrier diffusion, high carrier mobility, low carrier recombination rate, strong visible light absorption and novel electronic properties[19-22], due to the decrease in the dimension of materials and quantum confinement.

Recent researches have manifested that some 2D polarized materials with dipole moment induce vertical intrinsic electric field throughout the whole material, which implies promising

This article is protected by copyright. All rights reserved

Author Manuscript

excellent applications in photocatalytic water splitting[23-26]. The induced vertical intrinsic electric field not only efficiently separates carriers from interior to surface, but also effectively reduces the photocatalyst's band gap required for water splitting, leading to widened solar light absorption region[27]. Therefore, some 2D polarized materials have been theoretically and experimentally proved to be potential photocatalysts for water splitting. For example, Yang et al.[28] reported that the intrinsic electric fields in experimentally attainable 2D In_2Te_3 enhanced the performance for photocatalytic water splitting and the theoretical efficiency of solar to hydrogen using the full solar spectrum even achieved 32.1%. Liu et al.[22] experimentally confirmed that 2D material (WS_2 nanosheet) with dipole possessed full solar light spectrum photodegradation activity and high photocatalytic efficiency. Recently synthesized 2D Janus MXY (M=Mo, X/Y=S, Se, Te) are also potential photocatalyst for water splitting with a low carrier recombination rate due to structural symmetry breaking and induced internal electric field[25, 29-31]. Moreover, the switch of the dipole moment controlling by the stacking order indicates that asymmetric 2D Janus MXY (M=Mo, W, X/Y=S, Se, Te) are responsive to lights with a wide range spectrum from infrared to ultraviolet [24]. Our previous study[32] have demonstrated the blue phosphorene phase monolayer GeS and GeSe possess unique photocatalytic properties for water splitting and strain engineering can enhance photocatalytic activity under visible light due to the internal electric field induced by dipole moment from Ge atomic surface to S/Se atomic surface.

Although the 2D polarized materials possess promising potential application in photocatalysts of water splitting, however there's definitely room for improvement, considering the properties are limited by single material system. Recently many studies have shown that forming van der Waals (vdW) heterostructures based on different monolayers 2D materials is an effectively and facile way to combine the advantages of different 2D materials[33-36]. For example, Deng et al. reported that a photodetector based on MoS_2/black

This article is protected by copyright. All rights reserved

Author Manuscript

phosphorus vdW heterostructure showed a photodetection responsivity of 418 mA/W, which was much higher than the value of 4.8 mA/W for the single black phosphorus phototransistors[34]. Moreover, many recent studies have shown that constructing photocatalysts based on vdW heterostructures, such as GeS/WS_2[37], $GaS/g\text{-}C_3N_4$[38], MoS_2/ZnO[39], MoS_2/GaN[40], $MoS_2/g\text{-}C_3N_4$[41], $MoSe_2/SnS_2$[42], Blue $P/Mg(OH)_2$[43], Blue P/AlN[44], Blue P/BSe[45], BCN/C_2N[46], $\alpha\text{-}Fe_2O_3/g\text{-}C_3N_4$[47], can enhance the photocatalytic efficiency for water splitting[5, 18, 48, 49]. Considering the excellent advantage properties of the 2D polarized materials and the heterostructures for water splitting, exploring heterostructures based on the 2D polarized materials is a potential effective way to enhance the photocatalytic performance of water splitting process. Therefore, it is thus important and interesting to design and investigate the vdW heterostructures based on the 2D polarized materials.

Here, we design and investigate the vdW heterostructures based on the 2D polarized materials, using $GeS/MoSe_2$ as demonstration. GeS monolayer shared a similar hexagonal crystal structure and nearly identical lattice constants with $MoSe_2$ monolayer, which possesses sizable direct band gap, advantageous optoelectronic and distinguished mechanical properties. We expected that the advantageous properties of GeS and $MoSe_2$ were well preserved by forming the $GeS/MoSe_2$ vdW heterostructure. The structural stability, binding energy, internal electric field, opto-electronic properties and photocatalytic activity of the $GeS/MoSe_2$ heterostructure were systematically investigated via first principles calculations. The effect of biaxial strain on the properties of $GeS/MoSe_2$ vdW heterostructure was also discussed. The results suggest that the 2D polarized material based $GeS/MoSe_2$ vdW heterostructure is a potential novel high-efficiency photocatalyst for water splitting under a wide range from ultraviolet to near-infrared light.

2. **Results and discussion**

This article is protected by copyright. All rights reserved

Author Manuscript

The optimized lattice constants of GeS and $MoSe_2$ monolayers are 3.495 Å and 3.319 Å, respectively, agreeing well with previous study[32, 50-52]. The lattice constants difference between GeS and $MoSe_2$ monolayer, or the lattice mismatch, is about 2.4% which is in an acceptable range[53, 54] and good for constructing heterostructures along *z* direction. The stacking configuration of polarized material based heterostructure is more complex than that based on the non-polarized materials, because the GeS monolayer possesses a dipole induced internal electric field which is from Ge atomic surface to S atomic surface, indicating that both of the Ge atomic surface and S atomic surface should be considered to contact with the $MoSe_2$ monolayer when stacking the GeS/$MoSe_2$ heterostructures. As shown in Figure S1, twelve stacking structures of GeS/$MoSe_2$ heterostructures are considered, namely A1-, A2-, A3-, B4-, B5-, B6-, C7-, C8-, C9-, D10-, D11- and D12- stacking, respectively. In the A1-stacking, the Ge atomic surface approaches to the $MoSe_2$ monolayer and the GeS monolayer is directly stacked on the $MoSe_2$ of bottom layer, in which Ge atoms just locate above Mo atoms, and S atoms are just situated in the center of hexagon of the $MoSe_2$ monolayer. Moreover, the A2- and A3-stacking can be obtained as the $MoSe_2$ monolayer is translated along the vectors of ($b-a$) direction with the distance about 1/3 or 2/3 length of the unit cell, respectively, while the GeS monolayer is unchanged. Comparing to the A-combination, the direction of $MoSe_2$ monolayer in the B- combination is along opposite. The B1-, B2- and B3-stacking can be obtained as that the bottom layer $MoSe_2$ is rotated 180 degrees along the *z* direction from A3-, A1- and A2-stacking, respectively. The C-combination (D-combination) is similar to the A-combination (B-combination), respectively, while the $MoSe_2$ monolayer is directly stacked on the GeS of bottom layer, due to the S atomic surface is chosen to approach to the $MoSe_2$ monolayer.

In order to obtain the stable atomic configuration, all the twelve stacking are fully relaxed and the total energy of each stacking was calculated and counted. As shown in Figure

This article is protected by copyright. All rights reserved

Author Manuscript

S2, the B5-stacking gets the minimum value among the twelve stacking, indicating that B5-stacking is the most stable structure. Therefore, the B5-stacking (Figure 1 (a)) was chosen as the optimum representative stacking to show the properties of the GeS/$MoSe_2$ vdW heterostructure in the following. The energy as a function of lattice constant was shown in the Figure S3, the result indicates that the optimum lattice constant of GeS/$MoSe_2$ heterostructure is about 3.405 Å. To analyze the thermodynamic stability, the binding energy and phonon spectrum of GeS/$MoSe_2$ heterostructure were calculated. The binding energy E_d is calculated using the following definition:

$$= \frac{- \quad -}{A} \tag{1}$$

where E_h, E_{GeS} and E_{MoSe_2} represent the total energy of the GeS/$MoSe_2$ heterostructure, isolated GeS monolayer and isolated $MoSe_2$ monolayer, respectively, and A is the area of GeS/$MoSe_2$ heterostructure. A more negative binding energy indicates a more thermodynamically stable structure. The binding energy of GeS/$MoSe_2$ heterostructure is about -23.76 meVÅ^{-2}, which is close to those of other vdW heterostructures[39, 43, 55, 56], indicating that GeS/$MoSe_2$ heterostructure is thermodynamically stable. As shown in the Figure S4 and Figure S5, there is no imaginary vibration mode in the phonon spectrum of GeS/$MoSe_2$ heterostructure, confirming the dynamical stability of this structure.

The band structures of the isolated GeS, $MoSe_2$ monolayer and the GeS/$MoSe_2$ heterostructure were calculated based on the HSE06 method. As shown in Figure 1(b), the isolated GeS monolayer is an indirect semiconductor with a large band gap, and the Conduction Band Minimum (CBM) appears between the Γ and M points while the Valence Band Maximum (VBM) appears between the K and Γ points. The GeS monolayer has been reported as a potential promising photocatalyst for water splitting, due to a dipole moment induced vertical intrinsic electric field in the monolayer, which is helpful for separating of the

This article is protected by copyright. All rights reserved

Author Manuscript

carriers from interior to surface. However, the value of the band gap of the GeS monolayer is about 3.265 eV, similar to those of the conventional bulk material photocatalysts[8, 12], such as TiO_2, indicating that only the violet light, just about 5% of the total energy of the solar light, can be harvested, which greatly limits its applications.

The isolated $MoSe_2$ monolayer is a direct semiconductor with band gap about 1.889 eV, and both the CBM and VBM locate at the *K* point (Figure 1 (c)), in good agreement with previous results reported[51, 52]. The GeS/$MoSe_2$ heterostructure is a semiconductor with an indirect band gap, and the CBM and VBM locate at *Γ* point and *K* point respectively (Figure 1 (d)). The band structures of GeS/$MoSe_2$ heterostructure preserve both the properties of isolated GeS and $MoSe_2$ monolayer. The band gap of the GeS/$MoSe_2$ heterostructure is about 1.387 eV, which is smaller than those of the isolated GeS and $MoSe_2$ monolayer due to the formation vdW heterostructure. As a result, GeS/$MoSe_2$ heterostructure can harvest a broader light spectrum range from ultraviolet to visible solar light, comparing to that only ultraviolet light is harvested by the isolated GeS monolayer. Therefore, formatting GeS/$MoSe_2$ heterostructure is an efficient way to work out the problem that isolated GeS monolayer faced and to enhance solar light harvesting effectively.

What is more, the band structures for monolayer GeS, monolayer $MoSe_2$ and GeS/$MoSe_2$ heterostructure including the effect of spin-orbit coupling (SOC) were illustrated in Figure S6. It is clear seen that there is no significant SOC effect on the monolayer GeS, while there is a SOC effect on $MoSe_2$ and GeS/$MoSe_2$ heterostructure. It can be found that SOC slightly influences band gap values while maintaining the band-structure characteristics and shapes. In order to shed light on the fundamental mechanism of the orbital reconfiguration of the GeS/$MoSe_2$ heterostructure, the partial density of states (PDOS), the band decomposed charge density of the VBM and CBM were shown in Figure S7. It can be seen that it is *p*-orbitals of Ge, S and Se, and *d*-orbitals of Mo that contributed mainly to the VBM below Fermi level,

This article is protected by copyright. All rights reserved

Author Manuscript

while *p*-orbitals of Se and *d*-orbitals of Mo contributed mainly to the CBM above the Fermi level.

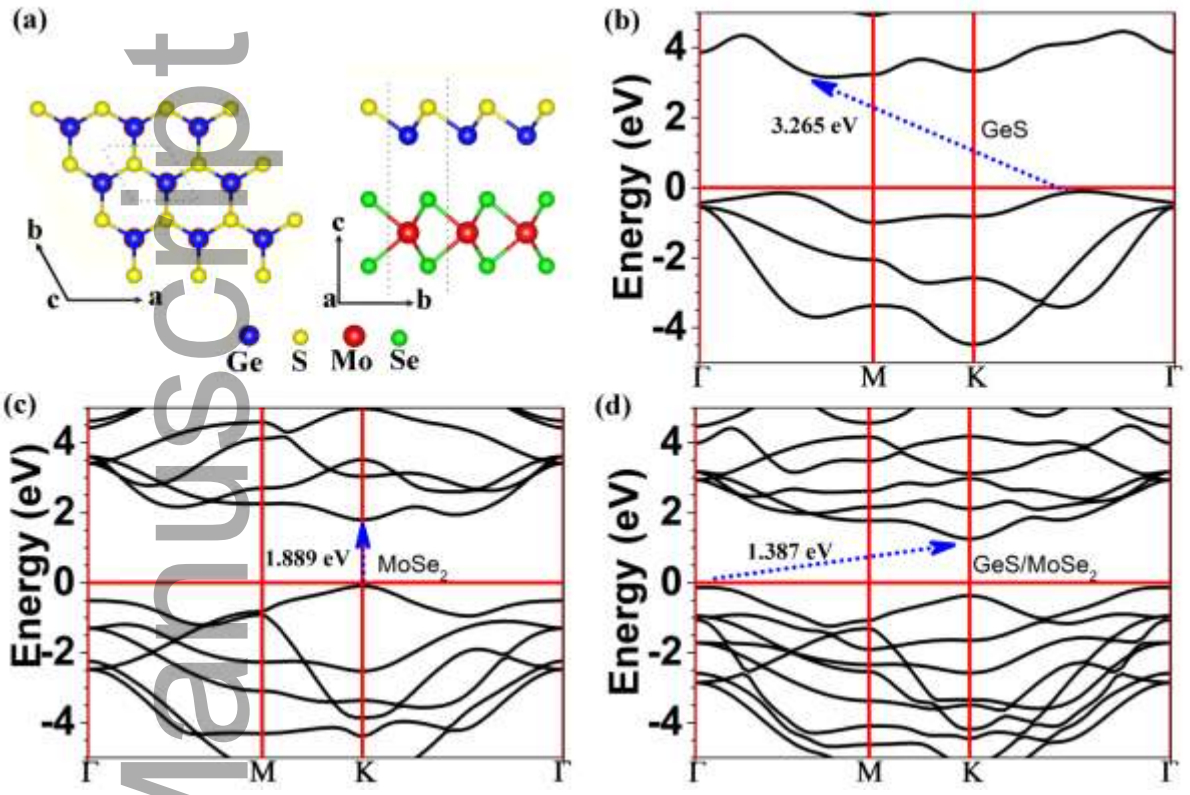

Figure 1. (a) Top and side views of optimum stacking order of the $GeS/MoSe_2$ heterostructure. The band structures (HSE06) of (b) monolayer GeS, (c) monolayer $MoSe_2$ and (d) $GeS/MoSe_2$ heterostructure.

Due to the charge redistribution, the 2D polarized materials possess an intrinsic dipole moment *P* through the materials. This intrinsic dipole moment *P* induces a surface potential difference ($\Delta\Phi$) between the vacuum levels of the top and bottom surface. As shown in the Figure 2 (a-c), for the isolated GeS monolayer, there is a $\Delta\Phi$ about 0.793 eV between bottom surface (Ge atomic side) and top surface (S atomic side) for the monolayer GeS. The direction pointing of the internal electric field (E_{eff}) is from bottom surface to top surface. As a contrast, the $\Delta\Phi$ is zero for $MoSe_2$ monolayer, due to the $MoSe_2$ monolayer is non-polarized 2D material with the same element on both sides. Importantly, for the $GeS/MoSe_2$ heterostructure, the surface potential difference $\Delta\Phi$ is considerable. The vacuum level of the bottom surface

This article is protected by copyright. All rights reserved

Author Manuscript

($MoSe_2$ monolayer side) is lower than that of the top surface (GeS monolayer side). As a consequence, there is an intrinsic electric field in the GeS/$MoSe_2$ heterostructure. The direction is from the bottom surface to the top surface, consistent to that of isolated GeS monolayer. Our result confirms that the GeS/$MoSe_2$ heterostructure preserves the properties of the dipole induced internal electric field, which is a distinct and advantageous property appeared in the 2D polarized materials. Furthermore, the value of the $\Delta\Phi$ of the GeS/$MoSe_2$ heterostructure is about 0.854 eV, larger than that of isolated GeS monolayer, suggesting that the band bending across the junction surface can be induced this surface potential difference.

To unveil the mechanism of the dipole induced internal electric field of the GeS/$MoSe_2$ heterostructure, the charge density difference and the plane-average charge density difference along the *z* direction of GeS/$MoSe_2$ heterostructure were calculated and plotted in Figure 2 (d) and Figure 2 (e), respectively. The charge density difference $\Delta\rho$ can be calculated according to the following equation

$$\Delta\rho = \rho \quad - \rho \quad - \rho \tag{2}$$

in which, $\rho_{heterostructure}$, ρ_{GeS} and ρ_{MoSe_2} are the charge densities of the GeS/$MoSe_2$ heterostructure, isolated GeS monolayer and isolated $MoSe_2$ monolayer with the same in-plane lattice constant, respectively. Moreover, the plane-average charge density difference along the *z* direction $\Delta\rho(z)$ can be obtained by integrating the in-plane charge density difference $\Delta\rho$ according to the following equation

$$\Delta\rho \quad = \int \rho \qquad - \int \rho \qquad - \int \rho \tag{3}.$$

Herein, yellow and blue isosurfaces correspond to charge accumulation and depletion, respectively. As shown in the Figure 2 (d) and Figure 2 (e), the Ge atom denotes electrons to the S atom, and the holes remained in the Ge atom, therefore the Ge atom gathers positive

This article is protected by copyright. All rights reserved

Author Manuscript

charges and the S atom gathers negative charges, confirming that the dipole induced internal electric field is from Ge atomic side to S atomic side which is mentioned above in Figure 2(a).

Moreover, the non-polarized $MoSe_2$ monolayer is unavoidably influenced by the polarized GeS monolayer, after forming the vdW GeS/$MoSe_2$ heterostructure. For the $MoSe_2$ layer, the charge redistribution behavior is regular. The electrons of each atom of the $MoSe_2$ layer transfer from further section to the nearer section which approaches to the GeS layer, leading to the polarization of electron and the formation of internal electric field induced by dipole moment. This means the dipole induced internal electric field appears in both the GeS layer and $MoSe_2$ layer of the GeS/$MoSe_2$ heterostructure. The direction pointing in the $MoSe_2$ layer is similar to that of the GeS layer. The dipole induced internal electric field of the GeS/$MoSe_2$ heterostructure is from the bottom surface to the top surface, which is consistent well with the result analyzed from the surface potential difference.

The 2D polarized material based GeS/$MoSe_2$ heterostructure preserves the advantageous properties, such as unique dipole induced internal electric field, as same as those of the 2D polarized GeS monolayer. The dipole induced internal electric field E_{eff} of GeS/$MoSe_2$ heterostructure is helpful for efficiency of separating carriers, reducing effectively the probability of recombination of photo-generated electron-hole pairs and ensuring the

Author Manuscript

This article is protected by copyright. All rights reserved

photocatalytic activity.

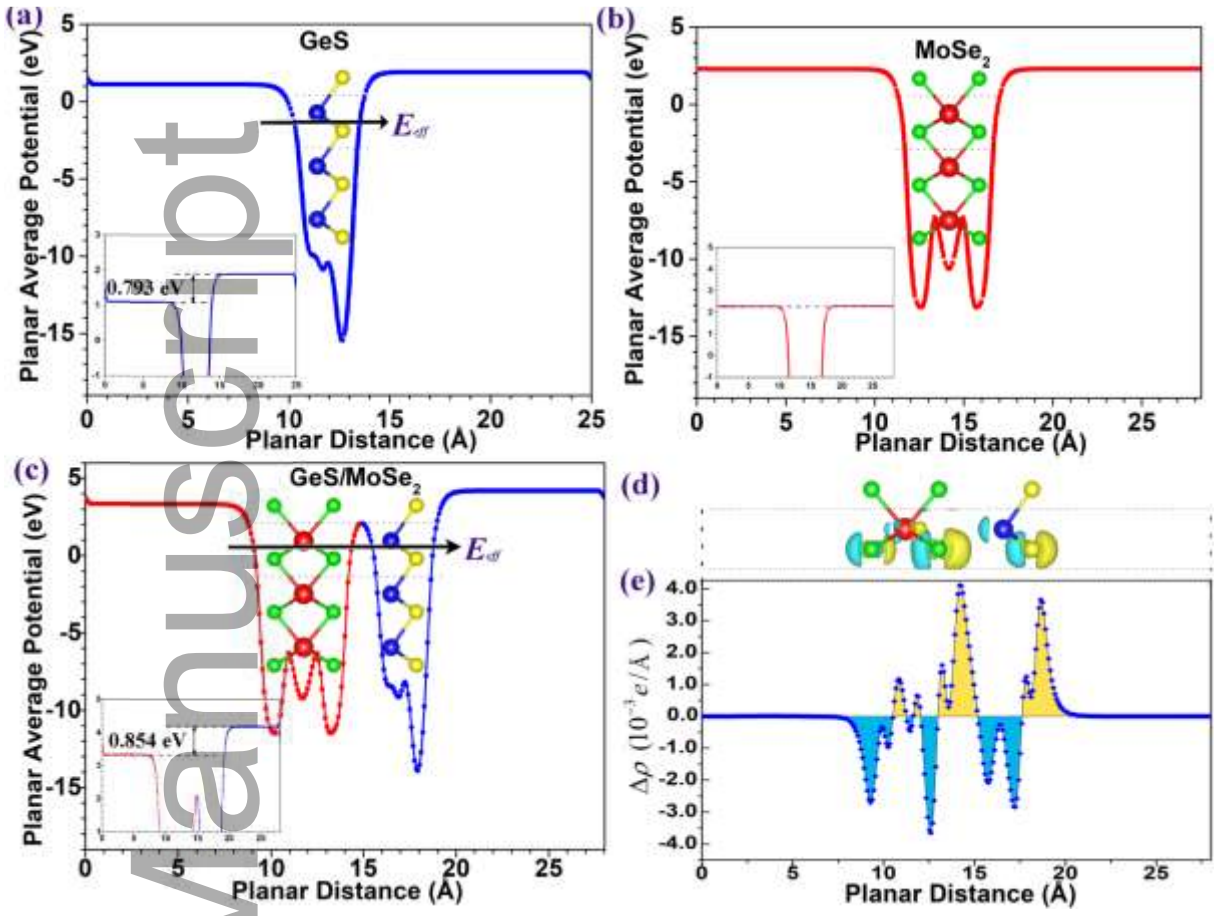

Figure 2. The planar average potential of (a) monolayer GeS, (b) monolayer $MoSe_2$ and (c) GeS/$MoSe_2$ heterostructure. (d) The charge density difference and (e) the plane-average charge density difference along the *z* direction of GeS/$MoSe_2$ heterostructure.

The solar light harvest is the premier step in the photocatalytic water splitting process, of which, the efficiency is a crucial factor. A desirable photocatalyst should possess not only strong solar light absorption ability, but also wide solar light adsorption range, especially visible light and infrared light. To elucidate the absorption performance, the absorption spectra were obtained by calculating the dielectric function according the following equation

$$\alpha(\omega) = \sqrt{}\,\omega\left(\sqrt{(\varepsilon(\omega))^2 + (\varepsilon(\omega))^2} - \varepsilon(\omega)\right) \quad (4)$$

In which, the absorption coefficient is represented by $\alpha(\omega)$, the real and imaginary parts of the frequency-dependent complex dielectric function correspond to $\varepsilon(\omega)$ and $\varepsilon(\omega)$,

This article is protected by copyright. All rights reserved

Author Manuscript

respectively. As shown in Figure 3 (a), the optical absorption coefficients as a function of wavelength for isolated GeS monolayer, isolated $MoSe_2$ monolayer and the GeS/$MoSe_2$ heterostructure were calculated. The isolated GeS monolayer only absorbs ultraviolet light, for which the proportion is just only about 5% of total solar light. The visible and infrared light that accounts for the most proportion of solar light cannot be utilized due to the large band gap of about 3.265 eV for GeS monolayer, leading to low solar absorption performance. As a contrast, the isolated $MoSe_2$ monolayer possesses excellent solar absorption performance, such as wide solar light adsorption ranging from the ultraviolet light to the visible light, strong solar light absorption ability and the absorption coefficients near to 10^6 cm^{-1}, agreeing well with the precious reported[57]. More importantly, vdW heterostructures can absorb solar light more efficiently than the isolated materials[57-59], as illustrated in the GeS/$MoSe_2$ heterostructure in this study. The excellent solar absorption performance of isolated $MoSe_2$ monolayer can be preserved in the GeS/$MoSe_2$ heterostructure. The absorption coefficient of the GeS/$MoSe_2$ heterostructure is slightly larger than that of the isolated $MoSe_2$ monolayer. In addition, as shown in Figure 3 (a) and Figure S8, the absorption edge of the GeS/$MoSe_2$ heterostructure has red shift to near infrared light, due to the band gap reduction to about 1.387 eV after formatting vdW heterostructure. The results of absorption spectrum suggest that GeS/$MoSe_2$ heterostructure possesses excellent solar absorption performance, which is contributed mainly by $MoSe_2$ monolayers. A wide light spectrum ranged from ultraviolet to near infrared light can be utilized with a high absorption coefficient, which is useful to enhance the solar energy conversion performance for water splitting.

In order to examine the possible applications of GeS/$MoSe_2$ heterostructure in the photocatalytic water splitting, the band alignments of the GeS/$MoSe_2$ heterostructure were compared with the redox potential of water. The dipole moment induced vertical intrinsic electric field in the 2D polarized materials will induce the energy level bend[27], reducing the

This article is protected by copyright. All rights reserved

Author Manuscript

photocatalyst's band gap requirement for water splitting. The energy alignment of GeS/$MoSe_2$ heterostructure was statistics according the methods using in the polarized materials as previous papers reported[23,25-27,32], in which the valence band maximum (VBM) was assumed to equal to the work function according the following equation:

$$= \phi \infty \quad - \tag{5}$$

where $\phi(\infty)$ is the electrostatic potential in vacuum, and is the Fermi energy level, and the conduction band minimum (CBM) was calculated according the following equation:

$$= \quad + \tag{6}$$

where E_{gap} is the value of band gap (HSE06).

As shown in the Figure 3 (b), the dipole moment induced vertical intrinsic electric field is from the bottom surface to the top surface, which is helpful to separate photo-generated electrons and holes effectively. Therefore, the electrons transfer from interior to the bottom surface, while the holes transfer from interior to the top surface, respectively. On the top side, the VBM is lower than the oxidation potential of O_2/H_2O (−5.67 eV), and the energy difference (ΔE_v) between VBM level and the oxidation potential level is 0.475 eV, which is suitable to drive holes to oxidize H_2O to O_2:

$$^{+} + \quad \rightarrow \quad + \quad ^{+} \tag{7}$$

On the bottom side, the CBM is higher than the reduction potential of H^+/H_2 (−4.44 eV), and the energy difference (ΔE_c) between CBM level and the reduction potential level of H^+/H_2 is 0.535 eV, which is suitable to urge electrons to catalyze H_2O to H_2:

$$^{-} + \quad \rightarrow \quad + \quad ^{-} \tag{8}.$$

In addition, the value of the ΔE_v is similar to that of ΔE_c, indicating a harmonious ability to produce hydrogen and oxygen. In general, the results suggest that GeS/$MoSe_2$ van der Waals heterostructure is a potential high-efficiency photocatalyst for water splitting thanks to

This article is protected by copyright. All rights reserved

Author Manuscript

it possesses a dipole moment induced vertical intrinsic electric field and a suitable band alignment under a wide range from ultraviolet to near-infrared light.

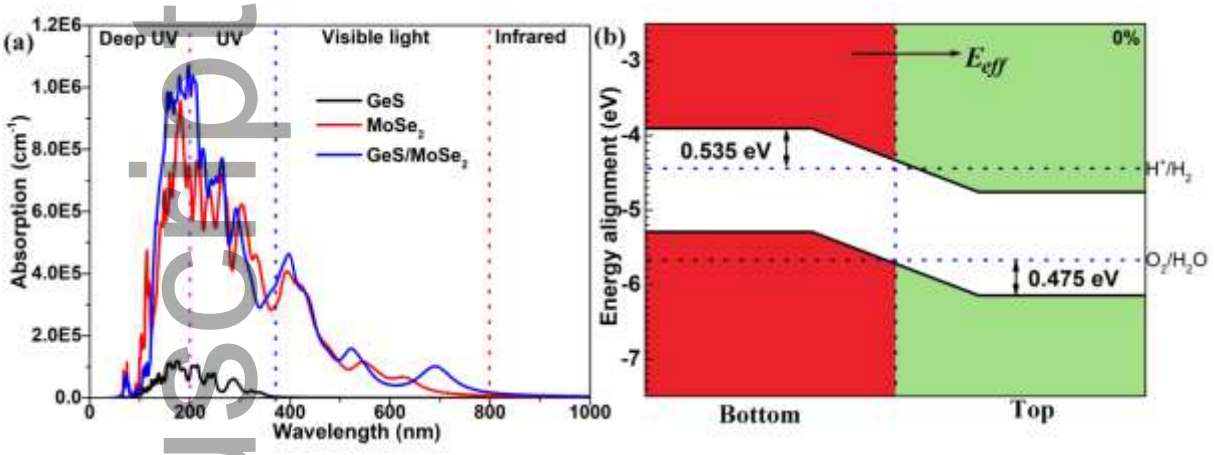

Figure 3. (a) Absorption coefficients of monolayer GeS, monolayer $MoSe_2$ and GeS/$MoSe_2$ heterostructure. (b) The energy alignment of GeS/$MoSe_2$ heterostructure.

Strain engineering is an effective and convenient strategy to tune the optoelectronic performance of 2D materials[51, 60-64]. Herein, the electronic, optical and photocatalytic properties of the GeS/$MoSe_2$ heterostructure under external biaxial strain were systematically investigated. Compressing and stretching are represented by symbol "-" and "+", respectively. The band structures (HSE06) of GeS/$MoSe_2$ heterostructure at various biaxial strain were shown in the Figure 4 (a-c) and the band gap as a function of biaxial strain range from 0 to ±10% was plotted in the Figure 4 (d). The magnitude of band gap for the GeS/$MoSe_2$ heterostructure can be tuned continuously by biaxial strain. For tensile strain, the band gap monotony decreased from 1.387 eV to 0.002 eV when the biaxial strain increased from 0 to +10%, indicating more visible light and infrared light can be harvested by GeS/$MoSe_2$ heterostructure, which also confirm by the absorption spectrum shown in Figure S9. For compressive strain, the band gap increases to the maximum 2.064 eV, when the biaxial strain

This article is protected by copyright. All rights reserved

Author Manuscript

decreased from 0 to -4%. The band gap decreased as the decrease of the biaxial strain from -4% to -10%.

Under compressive strain range of -2% to -3%, GeS/$MoSe_2$ heterostructure possesses a direct band gap character and the VBM and CBM both appear in the *K* point. More details are shown in the Figure 4 (b) and Figure S10, the CBMs and VBMs of GeS/$MoSe_2$ heterostructure at -2% and -3% biaxial strain are similar to that of monolayer $MoSe_2$. The lattice constants and band gap of GeS/$MoSe_2$ heterostructure at -2% (-3%) biaxial strain are 3.336 Å (3.302 Å) and 1.845 eV (1.968 eV), which are just close to 3.319 Å and 1.889 eV of monolayer $MoSe_2$, respectively, indicating the direct band gap character of GeS/$MoSe_2$ heterostructure mainly contributed by the monolayer $MoSe_2$. Therefore, it is feasible to tune the properties and enhance photocatalytic activity of GeS/$MoSe_2$ heterostructure via strain engineering.

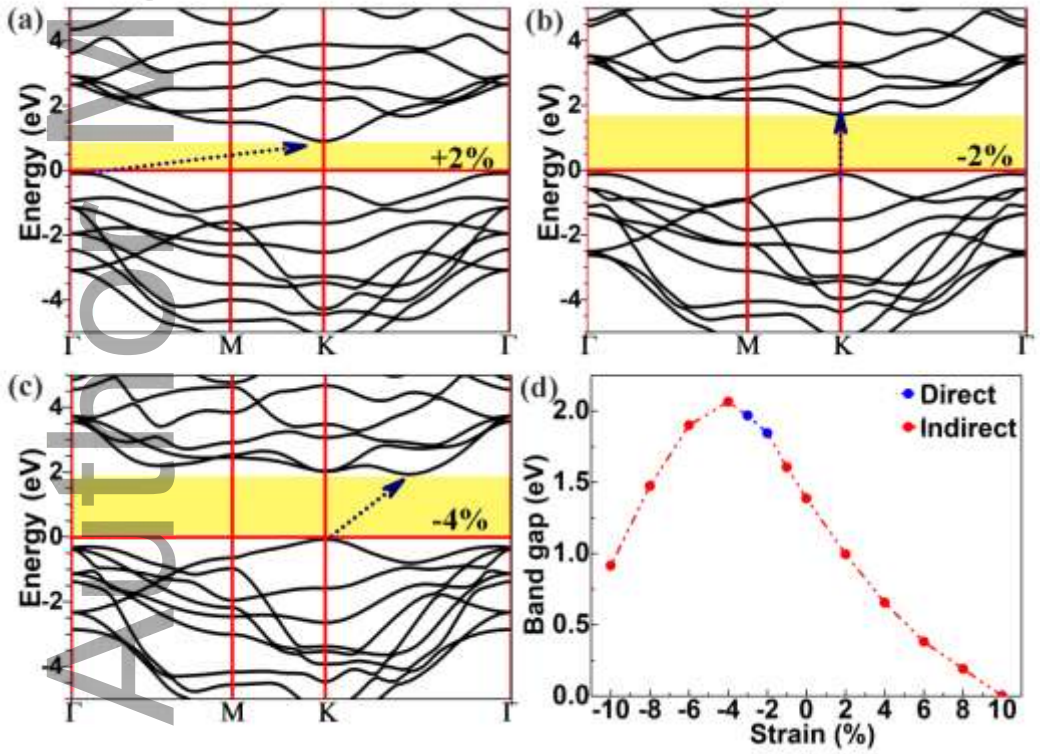

Figure 4. The band structures (HSE06) of GeS/$MoSe_2$ heterostructure at (a) +2%, (b) -2% and (c) -4% biaxial strain, respectively. (d) The band gap as a function of biaxial strain of GeS/$MoSe_2$ heterostructure.

This article is protected by copyright. All rights reserved

To make further inquiry into the possible applications in the photocatalytic water splitting, the band alignments of the GeS/$MoSe_2$ heterostructure under biaxial strain were plotted in Figure 5 and Figure S11. As shown in Figure 5 (a-c), when the biaxial strain is +2%, -2% and -6%, the GeS/$MoSe_2$ heterostructure possesses a suitable band alignment, in which the VBM is lower than the oxidation potential and the CBM is higher than the reduction potential. Conversely, as shown in Figure S11, when the biaxial strain is -10%, -8%, +4% and +6%, the CBM and VBM are not simultaneously consistent with the suitable redox potential of water. In order to elaborate the relationship between energy alignment and biaxial strain, the statistical data were obtained from the CBM on the bottom side and VBM on the top side of GeS/$MoSe_2$ heterostructure via various biaxial strain. As shown in Figure 5 (d), the GeS/$MoSe_2$ heterostructure possesses a suitable band alignment and possible applications in the photocatalytic water splitting in the strain range of -7%~+3%.

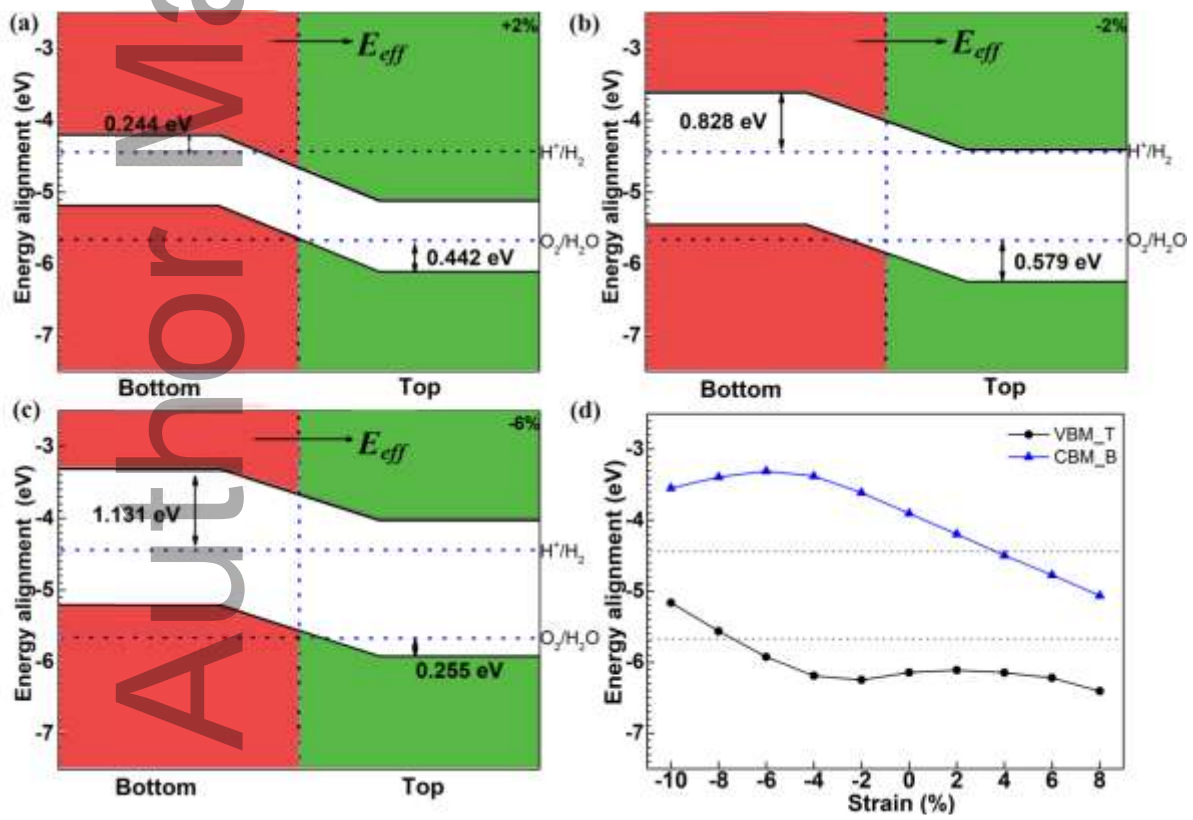

Author Manuscript

This article is protected by copyright. All rights reserved

Figure 5. The energy alignment of $GeS/MoSe_2$ heterostructure at (a) +2%, (b) -2% and (c) -6% biaxial strain, respectively. (d) The energy alignment as a function of biaxial strain of $GeS/MoSe_2$ heterostructure.

Author Manuscript

3. Conclusions

In summary, we propose a 2D polarized $GeS/MoSe_2$ vdW heterostructure for water splitting using full sunlight. The structural stability, binding energy, internal electric field, opto-electronic properties and photocatalytic activity of the $GeS/MoSe_2$ heterostructure were systematically investigated via first principles calculations. The results indicate that the advantageous properties of each material are well preserved in the $GeS/MoSe_2$ vdW heterostructure. The performance of $GeS/MoSe_2$ heterostructure is better than isolated materials, due to the properties of GeS monolayer and $MoSe_2$ monolayer are complementary by forming vdW heterostructure. Such as, the band gap of the $GeS/MoSe_2$ heterostructure is about 1.387 eV, which is helpful to harvest a broader light spectrum range from ultraviolet to visible light, comparing to that only ultraviolet light is harvested by the isolated GeS monolayer. The $GeS/MoSe_2$ heterostructure possesses a similar dipole induced internal electric field as that in GeS, with the direction pointing of the dipole induced internal electric field is from the bottom surface to the top surface. Such internal electric field reduces the probability of recombination of photo-generated electron-hole pairs effectively, and the photocatalyst's band gap requirement for water splitting. Furthermore, the $GeS/MoSe_2$ heterostructure possesses excellent solar absorption performance, which is contributed mainly by the isolated $MoSe_2$ monolayer. A wide light spectrum ranging from ultraviolet to near-infrared light can be utilized with a high absorption coefficient (10^6 cm^{-1}), which greatly enhanced the solar energy conversion efficiency for water splitting. The band alignments of the $GeS/MoSe_2$ heterostructure well satisfy the redox potential required for the water splitting

This article is protected by copyright. All rights reserved

reaction, indicating a harmonious ability to produce hydrogen and oxygen. In addition, it is feasible to tune the electronic and optical properties and enhances photocatalytic activity of $GeS/MoSe_2$ heterostructure via strain engineering. The biaxial compressive strain range of -2% to -3% induces the direct band gap character in $GeS/MoSe_2$ heterostructure. With the suitable band gap, dipole induced internal electric field, excellent solar absorption performance and suitable band alignments, 2D polarized material based $GeS/MoSe_2$ van der Waals heterostructure is a potential novel high-efficiency photocatalyst for water splitting under a wide range from ultraviolet to near-infrared light.

4. Computational methods

Vienna ab initio simulation package (VASP) in conjunction with the projector-augmented-wave (PAW) potential was used in all the calculations[65, 66]. The exchange-correlation energy was described by the Perdew-Burke-Ernzerhof (PBE) functional of the generalized gradient approximation (GGA). In order to obtain a more accurate band gaps, the HSE06 hybrid functional[67] was used. The van der Waals density functional of optB88[68-70] was considered to describe long-range vdW interactions to give an improved description for $GeS/MoSe_2$ vdW heterostructure. The energy cutoff for the plane-wave expansion of the wave function was set to 500 eV. All the structures were fully relaxed until satisfying an energy convergence of 10^{-6} eV and the maximum Hellmann Feynman force convergence of 0.001 eV/Å. The Gamma center scheme was used for the first Brillouin zone integration[71] with a fine grid of 8×8×1 and 11×11×1 for structure optimization and static calculation, respectively. The thickness of the vacuum region along the *z* direction was more than 20 Å to separate the artificial interactions due to the periodic image.

Supporting Information.

This article is protected by copyright. All rights reserved

Author Manuscript

Supplementary Figures of Figure S1-S11 for twelve stacking structures, Energy difference ΔE_i (eV), the energy as a function of lattice constant, the phonon spectrum, the band structures without (solid line) and with (dashed line) the spin-orbit coupling, the partial density of states (PDOS), the band decomposed charge density of the VBM and CBM, Absorption coefficients and the energy alignment of the GeS/$MoSe_2$ heterostructure, respectively.

AUTHOR INFORMATION

Corresponding Author

*E-mail: ouyangyf@gxu.edu.cn(Y.O.) qpeng.org@gmail.com (Q.P.)

COMPETING INTERESTS

The authors declare no competing financial interest.

ACKNOWLEDGMENTS

Authors acknowledge the financial support from National Natural Science Foundation of China (11464001).

DATA AVAILABILITY

All data generated or analyzed during this study are included in this published article and its supplementary information files.

Author contributions

D.G., Y.O., and Q.P. designed the project. D.G., X.T., H.C., and W.Z. carried out the simulations. D.G., X.T.,Y.D. and Y.O. done the analysis. D.G., Y.O., and Q.P. wrote the paper. All authors discussed and commented on the manuscript.

This article is protected by copyright. All rights reserved

Author Manuscript

Received: ((will be filled in by the editorial staff))
Revised: ((will be filled in by the editorial staff))
Published online: ((will be filled in by the editorial staff))

Author Manuscript

References

[1] A.J. Esswein, D.G. Nocera, *Chem. Rev.*, **2007**, *107*, 4022-4047.

[2] W. Lubitz, W. Tumas, *Chem. Rev.*, **2007**, *107*, 3900-3903.

[3] J. Liu, Y. Liu, N. Liu, Y. Han, X. Zhang, H. Huang, Y. Lifshitz, S.T. Lee, J. Zhong, Z. Kang, *Science*, **2015**, *347*, 970-974.

[4] W. Hu, J. Yang, *J. Mater. Chem. C*, **2017**, *5*, 12289-12297.

[5] C.F. Fu, X. Wu, J. Yang, *Adv. Mater.*, **2018**, *30*, 1802106.

[6] A. Fujishima, K. Honda, *Nature*, **1972**, *238*, 37-38.

[7] R. Asahi, T. Morikawa, T. Ohwaki, K. Aoki, Y. Taga, *Science*, **2001**, *293*, 269-271.

[8] W. Choi, A. Termin, M.R. Hoffmann, *J. Phys. Chem.*, **1994**, *98*, 13669-13679.

[9] U. Diebold, *Surf. Sci. Rep.*, **2003**, *48*, 53-229.

[10] H.G. Yang, C.H. Sun, S.Z. Qiao, J. Zou, G. Liu, S.C. Smith, H.M. Cheng, G.Q. Lu, *Nature*, **2008**, *453*, 638-641.

[11] K.M. Lee, C.W. Lai, K.S. Ngai, J.C. Juan, *Water Res.*, **2016**, *88*, 428-448.

[12] N. Daneshvar, D. Salari, A.R. Khataee, *J. Photochem. Photobiol., A*, **2004**, *162*, 317-322.

[13] M. Matsumura, S. Furukawa, Y. Saho, H. Tsubomura, *J. Phys. Chem.*, **1985**, *89*, 1327-1329.

[14] X. Zong, H. Yan, G. Wu, G. Ma, F. Wen, L. Wang, C. Li, *J. Am. Chem. Soc.*, **2008**, *130*, 7176-7177.

[15] K. Zhang, L. Guo, *Catal. Sci. Technol.*, **2013**, *3*, 1672.

This article is protected by copyright. All rights reserved

[16] K. Domen, A. Kudo, T. Onishi, *J. Catal.*, **1986**, *102*, 92-98.

[17] K. Domen, S. Naito, T. Onishi, K. Tamaru, *Chem. Phys. Lett.*, **1982**, *92*, 433-434.

[18] T. Su, Q. Shao, Z. Qin, Z. Guo, Z. Wu, *ACS Catal.*, **2018**, *8*, 2253-2276.

[19] X. Jiang, P. Wang, J. Zhao, *J. Mater. Chem. A*, **2015**, *3*, 7750-7758.

[20] Y. Jiao, L. Zhou, F. Ma, G. Gao, L. Kou, J. Bell, S. Sanvito, A. Du, *ACS Appl. Mater. Interfaces*, **2016**, *8*, 5385-5392.

[21] H.L. Zhuang, R.G. Hennig, *Chem. Mater.*, **2013**, *25*, 3232-3238.

[22] Y. Sang, Z. Zhao, M. Zhao, P. Hao, Y. Leng, H. Liu, *Adv. Mater.*, **2015**, *27*, 363-369.

[23] C. Fu, X. Li, Q. Luo, J. Yang, *J. Mater. Chem. A*, **2017**, *5*, 24972-24980.

[24] C. Xia, W. Xiong, J. Du, T. Wang, Y. Peng, J. Li, *Phys. Rev. B*, **2018**, *98*, 165424.

[25] Y. Ji, M. Yang, H. Lin, T. Hou, L. Wang, Y. Li, S.-T. Lee, *J. Phys. Chem. C*, **2018**, *122*, 3123-3129.

[26] Y. Ji, M. Yang, H. Dong, T. Hou, L. Wang, Y. Li, *Nanoscale*, **2017**, *9*, 8608-8615.

[27] X. Li, Z. Li, J. Yang, *Phys. Rev. Lett.*, **2014**, *112*, 018301.

[28] C. Fu, J. Sun, Q. Luo, X. Li, W. Hu, J. Yang, *Nano Lett.*, **2018**, *18*, 6312-6317.

[29] Y. Li, J. Wang, B. Zhou, F. Wang, Y. Miao, J. Wei, B. Zhang, K. Zhang, *Phys. Chem. Chem. Phys.*, **2018**, *20*, 24109-24116.

[30] Y. Liang, J. Li, H. Jin, B. Huang, Y. Dai, *J. Phys. Chem. Lett.*, **2018**, *9*, 2797-2802.

[31] X. Ma, X. Wu, H. Wang, Y. Wang, *J. Mater. Chem. A*, **2018**, *6*, 2295-2301.

[32] D. Gu, X. Tao, H. Chen, W. Zhu, Y. Ouyang, Q. Peng, *Nanoscale*, **2019**, *11*, 2335-2342

[33] A.K. Geim, I.V. Grigorieva, *Nature*, **2013**, *499*, 419-425.

[34] Y. Deng, Z. Luo, N.J. Conrad, H. Liu, Y. Gong, S. Najmaei, P.M. Ajayan, J. Lou, X. Xu, P.D. Ye, *ACS nano*, **2014**, *8*, 8292-8299.

Author Manuscript

This article is protected by copyright. All rights reserved

[35] V.D.S.O. Ganesan, J. Linghu, C. Zhang, Y.P. Feng, S. Lei, *Appl. Phys. Lett.*, **2016**, *108*, 122105.

[36] V.O. Ozcelik, J.G. Azadani, C. Yang, S.J. Koester, T. Low, *Phys. Rev. B*, **2016**, *94*, 035125.

[37] L. Ju, Y. Dai, W. Wei, M. Li, B. Huang, *Appl. Surf. Sci.*, **2018**, *434*, 365-374.

[38] B. Wang, A. Kuang, X. Luo, G. Wang, H. Yuan, H. Chen, *Appl. Surf. Sci.*, **2018**, *439*, 374-379.

[39] S. Wang, C. Ren, H. Tian, J. Yu, M. Sun, *Phys. Chem. Chem. Phys.*, **2018**, *20*, 13394-13399.

[40] Z. Zhang, Q. Qian, B. Li, K.J. Chen, *ACS Appl. Mater. Interfaces*, **2018**, *10*, 17419.

[41] Y. Yuan, Z. Shen, S. Wu, Y. Su, L. Pei, Z. Ji, M. Ding, W. Bai, Y. Chen, Z. Yu, Z. Zou, *Appl. Catal., B*, **2019**, *246*, 120-128.

[42] C.F. Fu, R. Zhang, Q. Luo, X. Li, J. Yang, *J. Comput. Chem.*, **2019**, *40*, 980-987.

[43] B. Wang, X. Li, X. Cai, W. Yu, L. Zhang, R. Zhao, S. Ke, *J. Phys. Chem. C*, **2018**, *122*, 7075-7080.

[44] Y. Qun, T. Chunjian, M. Ruishen, J. Junke, L. Qiuhua, S. Xiang, Y. Daoguo, C. Xianping, *IEEE Electron Device Lett.*, **2017**, *38*, 145-148.

[45] B. Wang, X. Li, R. Zhao, X. Cai, W. Yu, W. Li, Z. Liu, L. Zhang, S. Ke, *J. Mater. Chem. A*, **2018**, *6*, 8923-8929.

[46] R. Zhang, L. Zhang, Q. Zheng, P. Gao, J. Zhao, J. Yang, *J. Phys. Chem. Lett.*, **2018**, *9*, 5419-5424.

[47] X. She, J. Wu, H. Xu, J. Zhong, Y. Wang, Y. Song, K. Nie, Y. Liu, Y. Yang, M.T.F. Rodrigues, *Adv. Energy Mater.*, **2017**, *7*, 1700025.

[48] Y. Li, Y. Li, B. Sa, R. Ahuja, *Catal. Sci. Technol.*, **2017**, *7*, 545-559.

[49] P. Kumar, R. Boukherroub, K. Shankar, *J. Mater. Chem. A*, **2018**, *6*, 12876-12931.

[50] T. Hu, J. Dong, *Phys. Chem. Chem. Phys.*, **2016**, *18*, 32514-32520.

This article is protected by copyright. All rights reserved

Author Manuscript

[51] C. Chang, X. Fan, S. Lin, J. Kuo, *Phys. Rev. B*, **2013**, *88*, 195420.

[52] Y. Ding, Y. Wang, J. Ni, L. Shi, S. Shi, W. Tang, *Phys. B (Amsterdam, Neth.)*, **2011**, *406*, 2254-2260.

[53] S. Wei, F. Wang, P. Yan, M. Dan, W. Cen, S. Yu, Y. Zhou, *J. Catal.*, **2019**, *377*, 122-132.

[54] Y. Lin, H. Shi, Z. Jiang, G. Wang, X. Zhang, H. Zhu, R. Zhang, C. Zhu, *Int. J. Hydrogen Energy*, **2017**, *42*, 9903-9913.

[55] L. Peng, Y. Cui, L. Sun, J. Du, S. Wang, S. Zhang, Y. Huang, *Nanoscale Horiz.*, **2019**, *4*, 480-489.

[56] C. Xia, J. Du, W. Xiong, Y. Jia, Z. Wei, J. Li, *J. Mater. Chem. A*, **2017**, *5*, 13400-13410.

[57] Q. Peng, Z. Wang, B. Sa, B. Wu, Z. Sun, *Sci. Rep.*, **2016**, *6*, 31994.

[58] W. Zhang, L. Zhang, *RSC Adv.*, **2017**, *7*, 34584-34590.

[59] C. Xia, J. Du, X. Huang, W. Xiao, W. Xiong, T. Wang, Z. Wei, Y. Jia, J. Shi, J. Li, *Phys. Rev. B*, **2018**, *97*, 115416.

[60] D. Gu, X. Tao, H. Chen, Y. Ouyang, W. Zhu, Q. Peng, Y. Du, *Phys. Status Solidi RRL*, **2019**, *13*, 1800659.

[61] J. Feng, X. Qian, C.-W. Huang, J. Li, *Nat. Photonics*, **2012**, *6*, 866-872.

[62] N. Lu, H. Guo, L. Li, J. Dai, L. Wang, W.-N. Mei, X. Wu, X.C. Zeng, *Nanoscale*, **2014**, *6*, 2879-2886.

[63] Y. He, Y. Yang, Z. Zhang, Y. Gong, W. Zhou, Z. Hu, G. Ye, X. Zhang, E. Bianco, S. Lei, Z. Jin, X. Zou, Y. Yang, Y. Zhang, E. Xie, J. Lou, B. Yakobson, R. Vajtai, B. Li, P. Ajayan, *Nano Lett.*, **2016**, *16*, 3314-3320.

[64] Z. Fan, X. Jiang, Z. Wei, J. Luo, S. Li, *J. Phys. Chem. C*, **2017**, *121*, 14373-14379.

[65] G. Kresse, J. Furthmüller, *Phys. Rev. B*, **1996**, *54*, 11169-11186.

[66] P.E. Blochl, *Phys. Rev. B*, **1994**, *50*, 17953-17979.

This article is protected by copyright. All rights reserved

Author Manuscript

[67] J. Paier, M. Marsman, K. Hummer, G. Kresse, I.C. Gerber, J.G. Angyan, *J. Chem. Phys.*, **2006**, *124*, 154709.

[68] A.D. Becke, *Phys. Rev. A*, **1988**, *38*, 3098-3100.

[69] J. Klimeš, D.R. Bowler, A. Michaelides, *J. Phys.: Condens. Matter*, **2009**, *22*, 022201.

[70] J. Klimeš, D.R. Bowler, A. Michaelides, *Phys. Rev. B*, **2011**, *83*, 195131.

[71] H.J. Monkhorst, J.D. Pack, *Phys. Rev. B*, **1976**, *13*, 5188-5192.

Author Manuscript

This article is protected by copyright. All rights reserved

The performance of polarized GeS/$MoSe_2$ heterostructure is better than isolated material. GeS/$MoSe_2$ heterostructure possesses suitable band gap, dipole induced internal electric field, excellent solar absorption performance. The band alignments is suitable compared with the redox potential of water. GeS/$MoSe_2$ heterostructure is a potential novel high-efficienct photocatalyst for water splitting under a wide range of sunlight from ultraviolet to near-infrared.

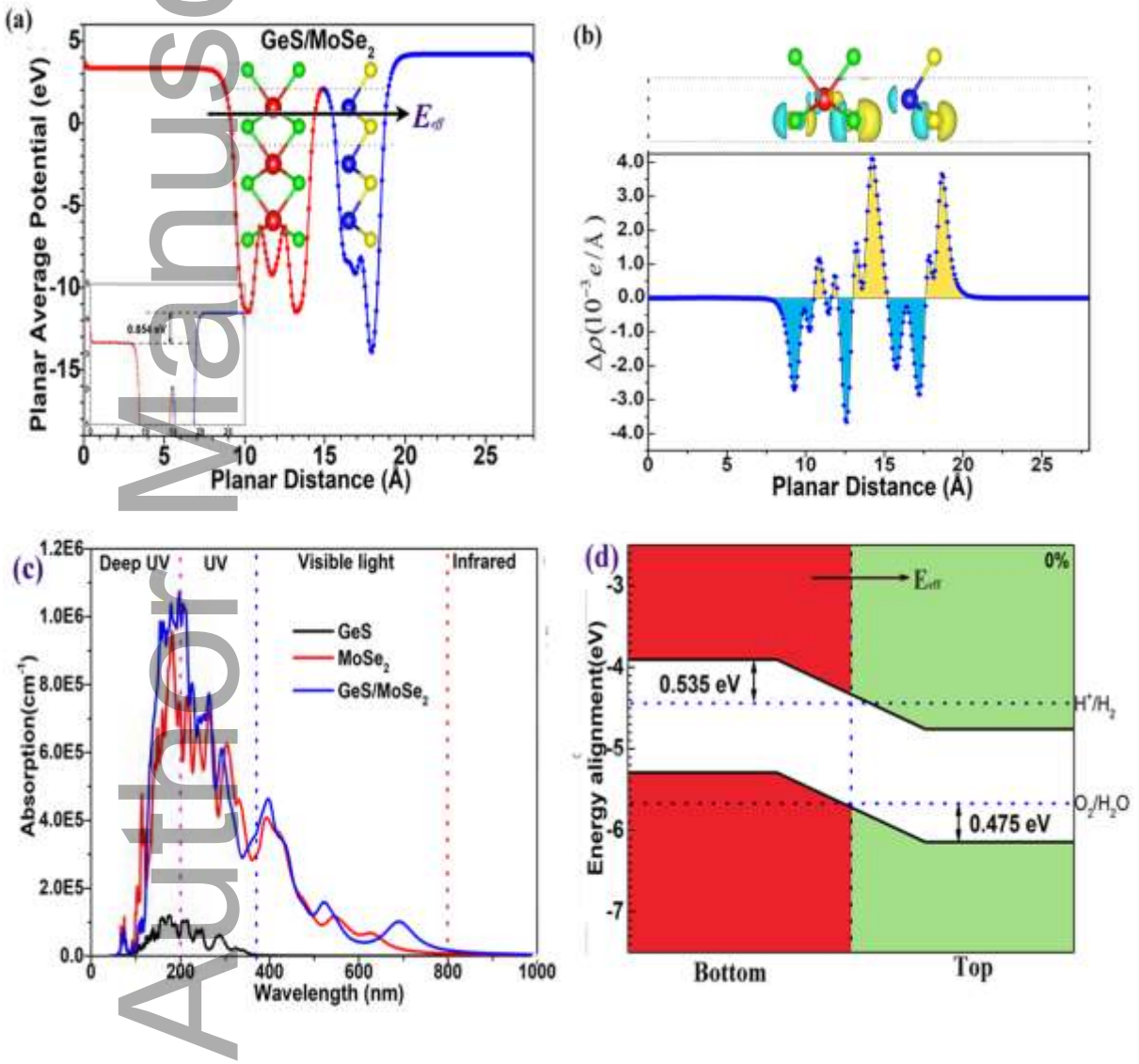

Author Manuscript

This article is protected by copyright. All rights reserved